J. Hydrau., Coast. Environ. Eng., JSCE, No. 733/II-63, 131-150, 2003 May

IMPACT OF CLIMATE CHANGE ON CIRCULATION PATTERNS IN THE JAPAN SEA

Olga TRUSENKOVA[1], Vladimir PONOMAREV[2] and Hajime ISHIDA[3]

[1] Ph.D., Senior Scientist, V.I. Il'ichev Pacific Oceanological Institute
(43 Baltiyskaya St., Vladivostok, Primorsky Krai, 690041, Russia)
[2] Ph.D., Leading Scientist, V.I. Il'ichev Pacific Oceanological Institute
(43 Baltiyskaya St., Vladivostok, Primorsky Krai, 690041, Russia)
[3] Member of JSCE, Dr. Eng., Professor, Dept. of Civil Engineering, Kanazawa University
(2-40-20 Kodatsuno, Kanazawa, Ishikawa, 920-8667, Japan)
E-mail:hishida@t.kanazawa-u.ac.jp

The study is motivated by new findings on oceanography of the Japan Sea and by research on climate change in the adjacent area. The primitive equation quasi-isopycnal model (MHI model) is applied to simulate principal circulation patterns in the Japan Sea for two different climatic conditions observed in the mid and late 20th century. It is shown that redistribution of the Tsushima Current transport between western and eastern branches and development of the subarctic gyre in the northwestern Japan Sea are controlled by variation of vertical density stratification and baroclinicity in the sea, in accordance with climate change in the East Asia - Northwest Pacific marginal area.

Key Words: *the Japan Sea circulation, numerical modeling, climate change, baroclinicity, the Tsushima Current branching*

1. INTRODUCTION

The Japan Sea is the East Asia marginal sea bounded by Siberia and Korea Peninsula in the west and the Sakhalin Island and Japanese Islands in the east. It is the deep sea, while straits connecting it to the adjacent ocean are shallow of about 50 – 150 m in depth. However, huge transport of warm and saline subtropical water estimated by more than 5×10^4 km^3 per year[1)] flows through the Japan Sea from the Tsushima (Korean) Strait to the Tsugaru and Soya (La Perouse) Straits (**Fig. 1a**). This thin layer (100 – 150 m) of warm and saline subtropical water lies on the top of about 3 km layer of cold and almost homogeneous deep and bottom water, usually called the Japan Sea Proper Water. Main thermocline and pycnocline is very thin in the Japan Sea, in comparison to the North Pacific ocean. It is no more than 400 – 500 m in depth in the southern area and even less in the northern area.

The bottom topography of the Japan Sea is complicated and features the deep Japan Basin in the northern sea with a trough extended to the Tatarsky Strait and the Ulleung and Yamato Basins separated by the underwater Yamato Rise and Korean Plateau in the southern sea. Seamounts such as the Bogorov Rise and Siberia Seamount are located in the western Japan Basin (**Fig. 1a**). Compared to other East Asian marginal seas, the Japan Sea has very narrow shelves, with the relatively extended shelf areas located off Vladivostok (Peter the Great Bay area), near the Tsushima Strait, and in the Tatarsky Strait. The shelf is extremely narrow at some locations near the Honshu coast and at the southwestern coast of Hokkaido (**Fig. 1a**).

The schemes of general circulation based on observation data had long been composed, such as Yurasov and Yarichin[2)]. The sea has both the warm subtropical and cold subarctic areas. In the southern subtropical sea area, branches of warm currents flow from the Tsushima Strait northward. The first (nearshore) quasi-barotropic branch of the Tsushima Current flows over the Japanese shelf, following the isobaths shallower 200 m, and the second (offshore) branch flows over the shelf break near Honshu Island with strong baroclinicity, accompanied by underlying countercurrent in the intermediate layers. This current develops mostly from spring to autumn[3)]. The East Korea Warm Current (EKWC; the third branch) flows along the Korea coast in the southwestern sea.

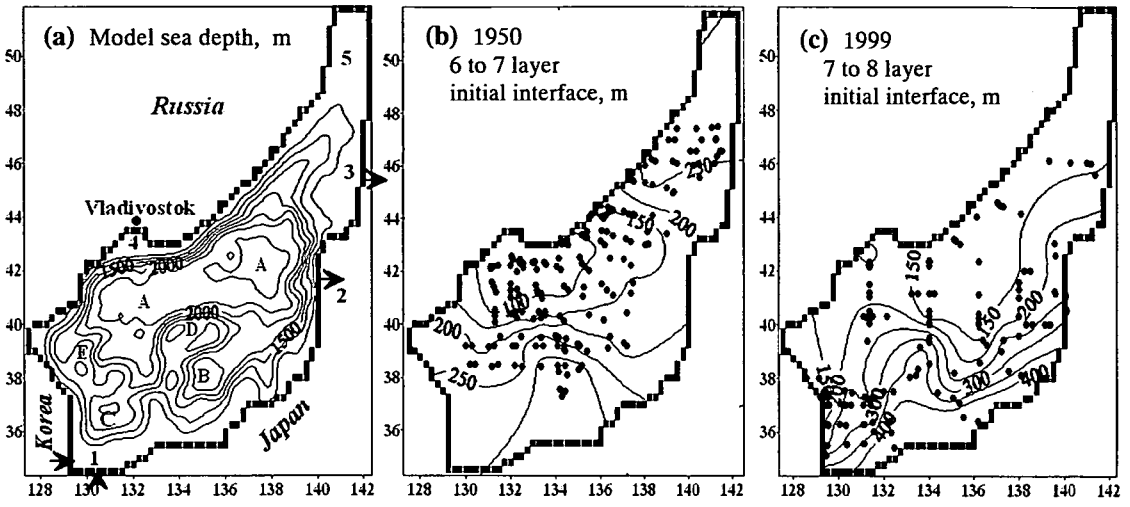

(a) Model sea depth (b)Station location in survey in 1950 (c) Station location in survey in 1999

Fig. 1 Model bottom topography (m) of the Japan Sea (a) and topography (m) of initial interfacial surface between two lower layers for the 1950 (b) and 1999 (c) Experiments. Contours are shown every 250 m in (a) and every 50 m in (b) and (c). The Tsushima Strait (1), Tsugaru Strait (2), La Perouse Strait (3), Peter the Great Bay (4), and Tatarsky Strait (5) are shown in (a). Topographic features shown in (a) are the Japan Basin (A), Yamato Basin (B), Ulleung Basin (C), Yamato Rise (D), and Korean Plateau (E). Station locations in the surveys in 1950 and 1999 are shown in (b) and (c), respectively.

The branches of the Tsushima Current manifest strong seasonal and interannual variability[3),4),5)]. Not all of them are necessarily present and they are even thought by some researchers to be meanders of the same current as a "single-meander-path-view" in the central southern sea over the Yamato Rise. Patterns of branching and meandering of the Tsushima Current in the southern Japan Sea were reviewed and investigated by Katoh[6)]. In particular, Katoh[6)] documented an anticyclonic meander and loop path of the EKWC in the southwestern Japan Sea. Seasonality of the EKWC was also studied; observational evidence that the current is intensified in summer and autumn, weakened or even absent in winter and spring is documented[4),5)].

The general circulation in the northwestern Japan Sea is cyclonic, with the cold Primorye (Liman) Current and North Korea Cold Current (NKCC) flowing south- and southeastward along the Russian (Siberian) coast and northern Korea Peninsula. The EKWC and NKCC meet and turn off the coast at approximately 37° – 39°N and flow across the sea. The subarctic (polar) frontal zone formed by their convergence separates the cold subarctic and warm subtropical areas. The southern front (the EKWC Extension) of the frontal zone is well known[2)]. The northern front (the NKCC Extension) has recently been documented[7)]. Northwestern thermal front[8)] was revealed in the area off southwestern Peter the Great Bay shelf, separating cold water spreading with the Primorye Current from the north and mixed water of the frontal zone. The closed cyclonic gyre between 41° – 43°N is documented both in the upper and deep layer, based on data from PALACE floats[9)].

Maximum kinetic energy of ocean/sea circulation is associated with mesoscale dynamics. Accordingly, mesoscale rings and eddies play an important role in formation of circulation and thermohaline structure in the Japan Sea. Their horizontal dimensions in the upper layer are of about 50 – 70 km, considerably larger than baroclinic Rossby radius of deformation, as estimated for the southern and, moreover, northern Japan Sea. Physical structure of mesoscale eddies in the southwestern Japan Sea was determined by Ichiye and Takano[10)]. Eddies were studied using satellite images, drifter data, mooring data, and ship measurements in the southeastern area along the Japanese coast[11)], in the southwestern area near the Ulleung Island[12),13)], in the East Korea Bay[14)], in the northwestern area off Vladivostok[15)], and in the Japan Basin interior[16),17)]. The Loop (anticyclonic) Path of surface warm water of the Tsushima Current was found in the central Japan Sea over Yamato Rise from infrared satellite images[18)].

Climate change around the Japan Sea has been intensely studied. Wintertime warming in the adjacent area has been documented in many studies;

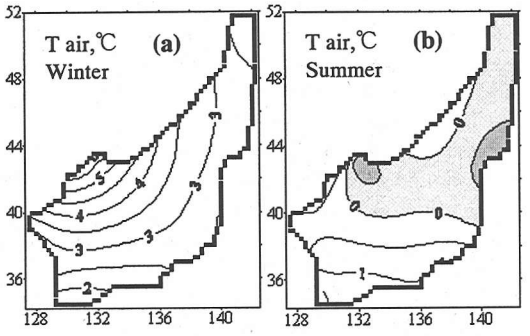

Fig. 2 Difference in surface air temperature (°C) over the Japan Sea from mid (1950) to late (1990) 20th century for January (a) and August (b). Contours are shown every 0.5°C. Area of negative values is in gray scale in (b).

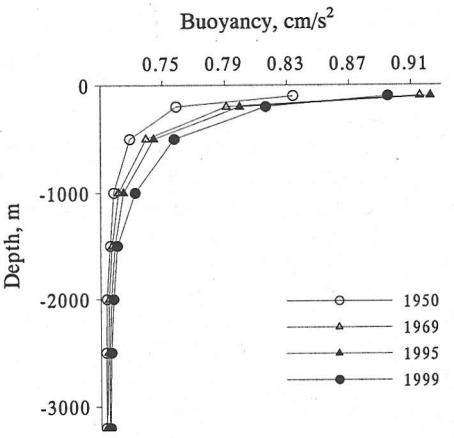

Fig. 3 Vertical buoyancy (cm/s^2) profiles (below 200 m) averaged for the northwestern Japan Sea in Peter the Great adjacent area, based on observation data in 1950 , 1969 , 1995 , and 1999.

review and original results are presented by Ponomarev et al.[19]. Wintertime increase of surface air temperature over the Japan Sea from 1950 to 1990 is shown in **Fig. 2a**, while no significant warming is observed in summer **(Fig. 2b)**. The potential temperature rise in different layers of the Japan Sea during late 20th century was found by Ponomarev and Salyuk[20]. It is higher in the main pycnocline than in deep layers, resulting in increase of vertical temperature and, therefore, density stratification[19]. **Fig. 3** shows stratification increase below 200 m from 1950 to 1999 in terms of buoyancy calculated from temperature profiles[19] and average salinity profile. (It is known that salinity variations in the intermediate and deep waters of the Japan Sea are low.) One can expect an impact of stratification change upon both large-scale and mesoscale circulation.

Many studies are devoted to numerical simulation of circulation in the Japan Sea. Principal physical mechanisms responsible for branching of the Tsushima Current in the southern sea area were numerically investigated[21]. It was shown that the eastern branches of the Tsushima Current are topographically steered, with the first (nearshore) branch characterized by strong barotropy throughout a year and baroclinic second (offshore) branch developed in summer and autumn, in agreement with observations[3].

The EKWC was originally considered as a permanent circulation feature - western boundary current controlled by β-effect[21]. Simulated seasonal changes in the EKWC are usually associated with increase (decrease) of the inflow through the Tsushima Strait in late summer – early autumn (late winter – early spring)[22]. However, observed seasonal and interannual variations of the EKWC can be also associated with redistribution of inflow transport through the Tsushima Strait between western and eastern branches. Cho and Kim[5] studied current branching in the Tsushima Strait numerically using a two-layer hydraulic model in a shallow channel. They showed that when inflow of cold intermediate water is prescribed to the strait from the north, northward flow along the western boundary of the strait channel is intensified in the upper layer, in agreement with observations. However, no reference was made to conditions in the sea outside the Tsushima Strait.

Wind stress is often considered as principal local forcing affecting circulation and, moreover, some models, such as NLOM model[23], are purely dynamical. However, it was shown that local thermal forcing only[24] or both wind and thermal forcing at the sea surface[25] can cause separation of the EKWC from the coast and formation of the cyclonic gyre in the northwestern Japan Sea. In recent studies modern primitive equation models are locally forced by both wind stress and buoyancy flux[22),26].

The purpose of this study is to simulate circulation patterns in the Japan Sea for climatic regimes of the mid and late 20th century associated with decreased and increased vertical density stratification in the sea. The MHI model developed in the Marine Hydrophysical Institute of National Academy of Science of Ukraine[27] is applied for the numerical experiments. In our opinion, setting up annual cycle of buoyancy forcing in the straits and at the sea surface is enough to explain principal difference between regimes of sea circulation in mid and late 20th century. No direct wind stress forcing is applied in the momentum equations for simulation of the current system.

2. NUMERICAL MODEL AND SIMULATION SETUP

(1) Application of the MHI hydrodynamic model to the Japan Sea

The MHI model is a primitive equation quasi-isopycnal model under hydrostatic, Boussinesq, β-plane, and free surface approaches. In isopycnal or layered models, the sea is represented by number of layers, mostly of uniform density, stacked one on another in the vertical. The layers are allowed to deform and interfacial surfaces are free to move vertically at every grid point. The model equations (momentum equations, equations for temperature and salinity, and continuity equations) are vertically integrated for each layer. Horizontal velocity and, in some models, temperature and salinity of each layer are allowed to vary horizontally.

In the MHI model, slip boundary condition and zero normal heat and salt fluxes are imposed at the seabed and closed lateral boundary. Velocity, layer thickness, and temperature and salinity of inflowing water are prescribed at an open lateral boundary. At the sea surface wind stress and kinematic condition for vertical velocity are set for the momentum equations. Heat balance condition at the sea surface, considering external atmosphere characteristics and sea temperature in the upper layer, is employed. It provides vertical heat flux to the upper mixed layer. Vertical freshwater flux is defined by evaporation and precipitation residual. Upper mixed layer model is employed[28]. Restoration to prescribed surface temperature and salinity is not mandatory but upper layer salinity is very sensitive to precipitation data.

As in any isopycnal model, simulation of winter convection, fronts, and jet currents is facilitated by layer outcropping (vanishing) device. In the MHI model buoyancy is allowed to vary horizontally within inner layers, as well as in the upper layer. Approximation of subduction and of lateral mixing of water with different temperature and salinity is facilitated by this approach. In order to maintain stable vertical stratification "base" buoyancy is introduced, constraining buoyancy variations in inner layers, while buoyancy in the upper layer is unbounded. Namely, it is postulated that:

$$b^{bas}_k \le b_k < b^{bas}_{k-1} \quad \text{for } k > 1, \qquad (1)$$

where $k = 1, \ldots, N$ is layer number from sea surface (k=1) to seabed (k=N), N is number of layers, b_k is buoyancy in the kth layer, b^{bas}_k is base buoyancy of the kth layer: $b^{bas}_k < b^{bas}_{k-1}$, $b^{bas}_1 = \infty$, $b^{bas}_N = 0$. An inner layer outcrops (vanishes) if buoyancy gets out of its base limits. In this case water goes to an adjacent layer of appropriate base buoyancy. Buoyancy is defined as follows:

$$b_k = g(\rho - \rho_k)/\rho, \qquad (2)$$

where $g = 980$ cm/s^2 is gravity acceleration, ρ_k is density in the kth layer, $\rho = 1.02815$ g/cm^3 is reference (maximum) density.

It is important to note that scale-selective bi-harmonic rather than harmonic viscosity is applied in the momentum equations. Harmonic viscosity is switched on only when needed to suppress checkerboard noise. Equivalent harmonic viscosity can be estimated according to Semtner and Mintz[29]:

$$A^{eq}_h = 4A / (\delta x)^2, \qquad (3)$$

where A is bi-harmonic viscosity coefficient, A^{eq}_h is equivalent harmonic viscosity coefficient, and δx is horizontal grid dimension. Coefficient of diapycnal mixing μ_k at an interface between kth and (k+1)th layers can be related to harmonic diapycnal mixing coefficient κ_h through thickness of adjacent layers:

$$\kappa_h = \mu_k(h_k + h_{k+1})/2, \qquad (4)$$

where h_k and h_{k+1} are thickness of adjacent layers[27].

Model bottom topography is introduced by scaling sea depth:

$$H'(x,y) = H_m + \alpha(H(x,y) - H_m), \qquad (5)$$

where H_m is mean sea depth, α is scaling factor ($0 < \alpha < 1$), and H(x,y) and H'(x,y) are initial and scaled sea depth, respectively. Note, that average sea depth is not changed by this transform. Scaled sea depth is smoothed with 9-point linear filter.

In case of unstable density stratification conventional convective adjustment procedure is employed, considering base stratification. The basic assumptions, governing equations, finite difference approximation, and methods of numerical solution are described in detail by Shapiro[27].

The model domain of the Japan Sea extends from 34°20′ to 51°50′N in the south-north direction and from 127°20′ to 142°20′E in the west-east direction. The major ports are the Tsushima, Tsugaru, and Soya (La Perouse) Straits (**Fig. 1a**). The horizontal resolution of 1/8° (10 km in the west-east direction and 14 km in the south-north direction) allows us to resolve mesoscale circulation features with typical dimensions of about 40 – 100 km[13),15),16),17]. Vertical resolution is 7 or 8 layers, representing upper mixed layer, pycnocline, and Japan Sea Proper Water.

Bottom topography is taken from navigation maps. Smoothed coastline (**Fig. 1a**) and scaling factor $\alpha = 0.5$ for bottom topography correspond to the horizontal resolution employed. Noto Peninsula and Sado Island are neglected in coastline but they are represented in bottom topography as spurs at (137°E, 37°–38°N) and (138°30′E, 38°–38°30′N), respectively. Therefore, they affect circulation. High horizontal resolution, such as that applied by Hogan and Hurlburt[23], is needed to represent islands explicitly.

The Japan Sea shelves cannot be realistically represented with the scaling factor assumed but topography slopes are represented. It is sufficient for the present horizontal resolution, as the shelf areas in the Japan Sea are very limited.

Equivalent isopycnic harmonic viscosity of 100 m^2/s, as calculated from employed bi-harmonic viscosity of 5×10^9 m^4/s (Eq. 3), is moderate in value, facilitating resolution of mesoscale structures. Diapycnal mixing is set very low: $5\cdot10^{-6}$ cm/s corresponds to $2\times10^{-2}cm^2/s$ for a 100 m thick layer (see Eq. 4).

(2) Design of numerical experiments

Two short-term experiments are performed in this study, associated with climatic regimes of early 1950s (decreased vertical stratification in the sea) and late 1990s (increased stratification). They are called the 1950 Experiment and 1999 Experiment, respectively. Time step is 5 min in both cases. Vertical resolution is 7 layers in the first case and 8 layers in the second case. The base stratification is taken from average vertical density profile in the sea (**Table 1**).

Initial conditions for the experiments are based on temperature and salinity data of the 3rd cruise of R/V "Vityaz" in January – February, 1950 (about 180 stations) and of the cruises of R/V "Roger Revelle" and R/V "Professor Khromov" in June – August, 1999 (more than 200 stations). Both surveys cover most of the Japan Sea but in few areas data are scarce (**Figs. 1b** and **1c**). To reduce possible errors we chose to interpolate initial isopycnal topography rather than temperature and salinity fields. Isopycnal surfaces corresponding to base buoyancy are taken as initial lower interfaces of the layers at every hydrographic station. Stations located within synoptic eddies are excluded from the dataset, providing large-scale smoothing.

Gridded interfaces are smooth and continuous in the interpolated and extrapolated areas. They have similar large-scale features in 1950 and 1999. These features are an elevation associated with the cyclonic gyre in the northwestern Japan Sea and Tatarsky Strait and depression in the southern subtropical area, as seen in topography of interface between two lower layers (**Figs. 1b** and **1c**). This isopycnic surface with buoyancy of 0.8 cm/s^2 represents a pycnocline bottom (boundary between intermediate and deep waters). Other interfaces have similar topographic features.

Stratification increase associated with climate change from 1950 to 1999 manifests itself in deepening of the pycnocline bottom in 1999, compared to 1950, especially in the subarctic area well covered with observations. The center of the cyclonic gyre is shifted northeastward in 1999, compared to 1950 (**Figs. 1b** and **1c**). Reasonable initial interface topography obtained justifies procedures accepted for handling observation data and lays grounds for steady simulations. Initial layers are of constant density (isopycnal layers), so that initial lateral density gradient in the sea is set by the interface slopes.

Table 1 Simulation parameters

Base buoyancy, cm/s^2 for 1950 Experiment	∞, 2.0, 1.6, 1.3, 1.0, 0.8, 0
Base buoyancy, cm/s^2 for 1999 Experiment	∞, 2.4, 1.8, 1.4, 1.05, 0.87, 0.81, 0
Volume transport in the Tsushima Strait	3Sv/2Sv for August/February
Temperature and salinity of water entering the Western Tsushima Channel	1st layer: 23°C / 14°C; 32 psu / 34.6 psu for August/February
	2nd layer: 21°C / 14°C; 33.5 psu / 34.6 psu for August/February
	3rd layer: 14°C / 14°C; 34.3 psu / 34.6 psu for August/February
Temperature and salinity of water entering the Eastern Tsushima Channel	1st layer: 23°C / 14°C; 33.5 psu / 34.65 psu for August/February
	2nd layer: 21°C / 14°C; 34.2 psu / 34.65 psu for August/February
	3rd layer: 14°C / 14°C; 34.65 psu / 34.65 psu for August/February

In the momentum equations wind stress at the sea surface is set up equal to zero. For heat balance condition at the sea surface, net downward radiative flux is taken from climatology the same for both experiments. Constant wind speed of 5 m/s is employed in the upper layer model and heat balance equation at the sea surface. Freshwater flux at the sea surface is set equal to zero. External atmosphere characteristics specific for the chosen climatic regimes is monthly mean air temperature averaged for 1949 – 1950 and 1989 – 1990, respectively.

The Western and Eastern Tsushima Channels are set as inflow ports equally dividing inflow transport (**Table 1**). Outflow ports are the Tsugaru Strait and Soya (La Perouse) Strait, with the outflow transport divided in ratio of 2:1 between them. Transport through the northern boundary of the Tatarsky Strait is usually considered insignificant and is neglected in these experiments, as well as river discharge (**Fig. 1a**). As the straits connecting the Japan Sea with adjacent basins are shallow (about 100 m), water flows in and from the sea through the upper 3 layers. Annual cycle of volume transport through the Tsushima Strait and of inflowing water temperature and salinity is based on observation data[1),30)]. They are intentionally taken the same for both experiments and approximated by sinusoid from prescribed extreme values (**Table 1**).

3. SIMULATION RESULTS

(1) Circulation change of the Tsushima Current in the southern Japan Sea

In the numerical experiments performed, an influence of wind stress on sea currents is neglected and the annual cycle of circulation in the Japan Sea is simulated under seasonally varied buoyancy forcing only. Circulation patterns are conditioned by the Japan Sea geometry and bottom topography. Principal currents of the Japan Sea obtained in these experiments are consistent with earlier simulation results and observations discussed in Section 1.

For the 1950 and 1999 Experiments, surface currents for summer are shown in **Figs. 4a** and **5a**, respectively, and for winter in **Figs. 4c** and **5c**, respectively. Currents in the pycnocline are shown in **Figs. 4b** and **5b**. As seen from **Figs. 4** and **5**, in the southern Japan Sea, warm currents carrying subtropical water from the Tsushima Strait to the north are simulated in both experiments. At the same time, difference in circulation for the climatic regimes of mid and late 20th century can be clearly seen from **Figs. 4** and **5**, as will be discussed below.

Depths of interfacial surfaces are shown for layers corresponding to the upper portion of pycnocline (**Figs. 6a** and **7a**) and to the pycnocline bottom (**Figs. 6b** and **7b**). As seen from **Figs. 6** and **7**, the subtropical area of warm currents is characterized by large-scale depression of interfaces, as pycnocline is relatively thick there.

As simulated in both experiments, inflow transport entering the sea through the Western Tsushima Channel splits, with the East Korea Warm Current (EKWC) originating from the portion of it and flowing northward along the Korean coast in the upper layers (**Figs. 4** and **5**). The simulated EKWC is intensified in summer (in seasonal conditions of increased baroclinicity; **Figs. 4a** and **5a**), compared to winter (decreased baroclinicity; **Figs. 4c** and **5c**), in agreement with observations[5]. The same principal difference is revealed in comparison of the 1950 and 1999 Experiments. The current turns eastward and separates off the coast at 37°–38°N in summer 1950 (in climatic conditions of decreased baroclinicity; **Fig. 4a**) and at 39°30′N in summer 1999 (increased baroclinicity; **Fig. 5a**). The EKWC is completely absent in winter 1950 (the weakest vertical stratification; **Fig. 4b**). Episodic absence of the EKWC was earlier reported from observations[4]. Velocity in the upper layers within the EKWC is higher in 1999, compared to 1950: 17.5 cm/s versus 12.5 cm/s for the velocity profile (**Fig. 8a**) at the location 1 from **Figs. 4a** and **5a**. Pycnocline deepens in 1999 after 2 years of integration, compared to pycnocline for both 1999 initial condition and for 1950 after 2.5 years of integration (**Fig. 8b**).

In 1999 the EKWC is so strong that it develops an anticyclonic recirculation gyre and multiple mesoscale rings in the western sea area (**Fig. 5**). A looping pattern of the EKWC in the southwestern Japan Sea was documented by Katoh[6] and simulated by Kim and Yoon[22] but it extends much farther northward, as simulated in summer 1999 (**Fig. 5a**). In this area depression associated with the subtropical circulation can be seen in the layer interfaces in 1999 (**Fig. 7**), while in summer 1950 elevation typical for the subarctic gyre extends there (**Fig. 6**). Presence of the pool of warm surface water and development of the pycnocline anticyclonic eddies in the northwestern Japan Sea is supported by observational evidence from infrared satellite imagery and ship and drifter data[13),14),15),17),31)].

A countercurrent is simulated underneath the EKWC in the intermediate layers (**Figs. 4b** and **5b**). It is known from observation data analysis and was earlier reproduced by numerical models[22),26)]. As simulated in both experiments, its core, associated with intermediate velocity maximum, is deepened and velocity in it is higher in 1950, compared to 1999: maximum velocity is of 8 cm/s at 150 m depth in 1950 and of 5 cm/s at 110 m depth in 1999 (**Fig. 8a**).

Simulation results show that portion of inflow through the Western Tsushima Channel turns eastward and converges with the inflow through the Eastern Channel, forming eastern branches of the Tsushima Current, well known from observations[3]. Numerical models mostly reproduce the only nearshore or offshore branch along the Japanese coast[22),23),26)]. Yoon[21] numerically studied the first (barotropic) and second (baroclinic) branches by analyzing baroclinic velocity component separately.

Similar pattern is obtained in the 1950 experiment (**Fig. 4a**), probably due to insufficient horizontal resolution and scaled bottom topography (see Section 2). In this experiment most of inflow through the Tsushima Strait goes to the east. The current along the coast of Honshu Island meanders with bends of bottom topography. In particular, anticyclonic meanders develop over the spurs at (137°E, 37°–38°N) and (138°30′E, 38°–38°30′N) associated with the Noto Peninsula and Sado Island, although they are absent in the coastline, as was discussed in Section 2. These meanders are clearly seen in the pycnocline (**Fig. 4b**). Similar pattern is simulated in the intermediate layer in the 1999 Experiment (**Fig. 5b**).

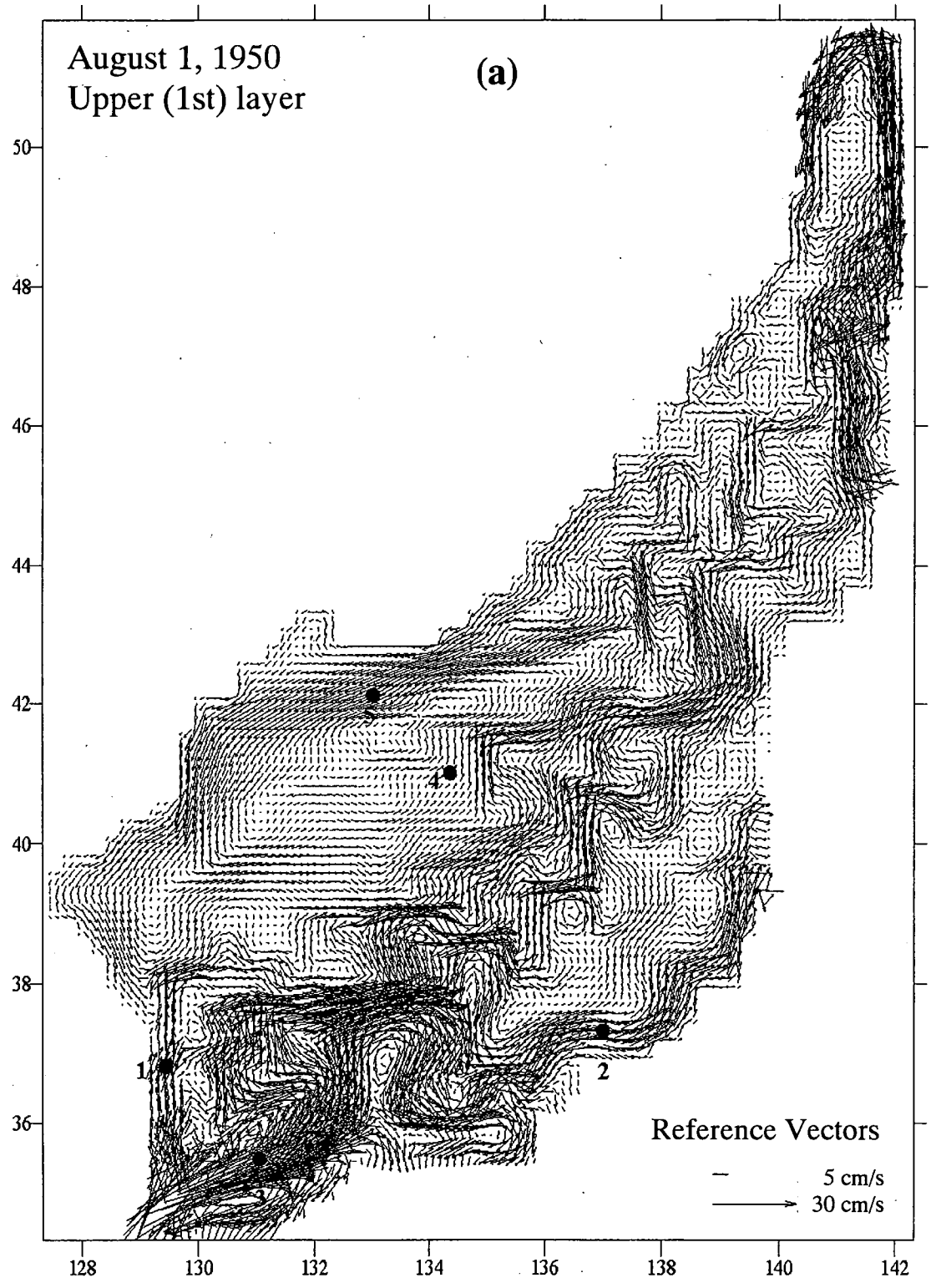

Fig. 4 The 1950 Experiment. Horizontal velocity (cm/s) for the 3rd year of integration in the upper (a) and 6th (b) layers on August 1 and in the upper layer on February 1 (c). Grid locations for vertical profiles in Fig. 8 (for 1950) are shown in (a).

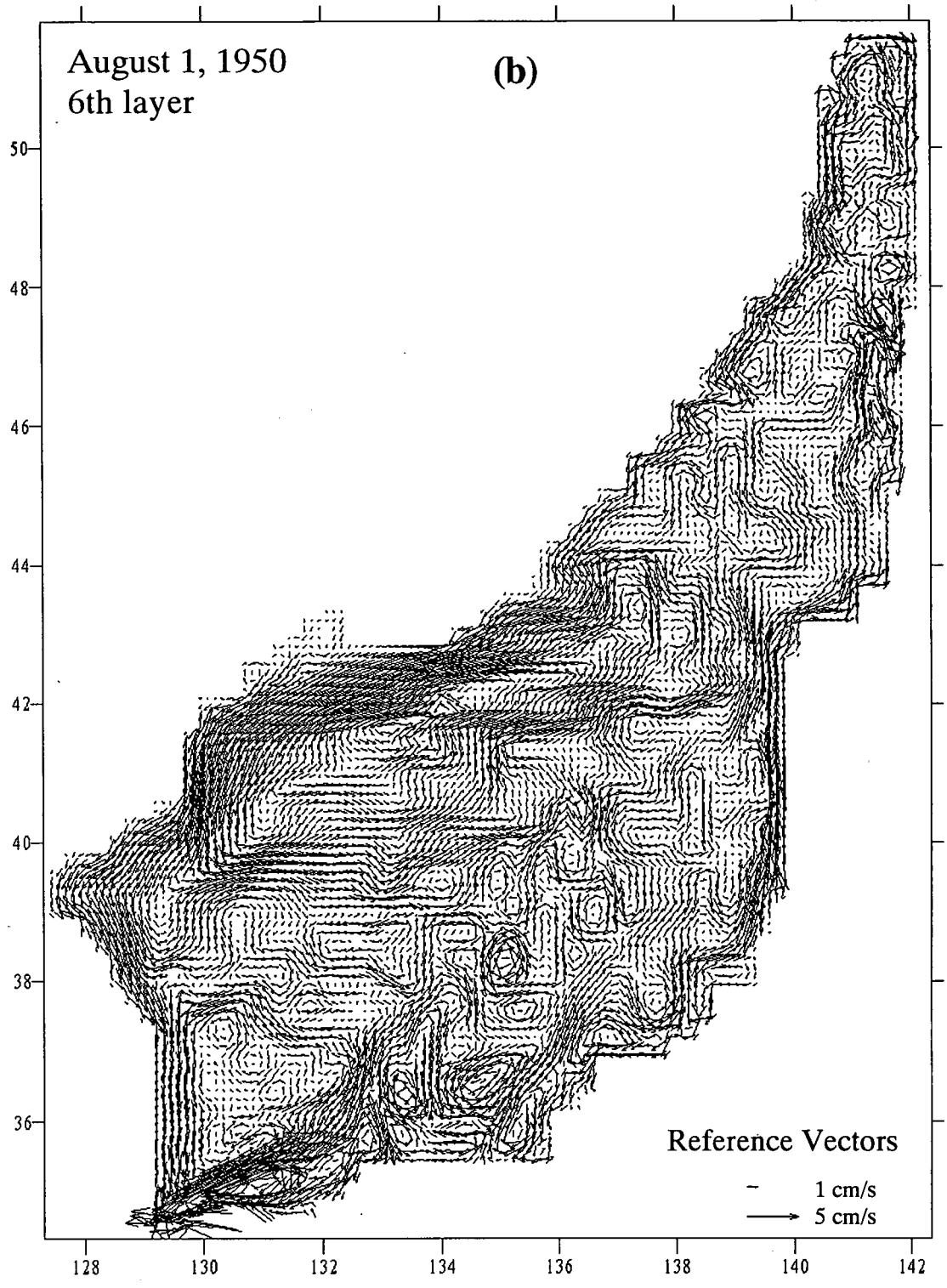

Fig.4 (continued).

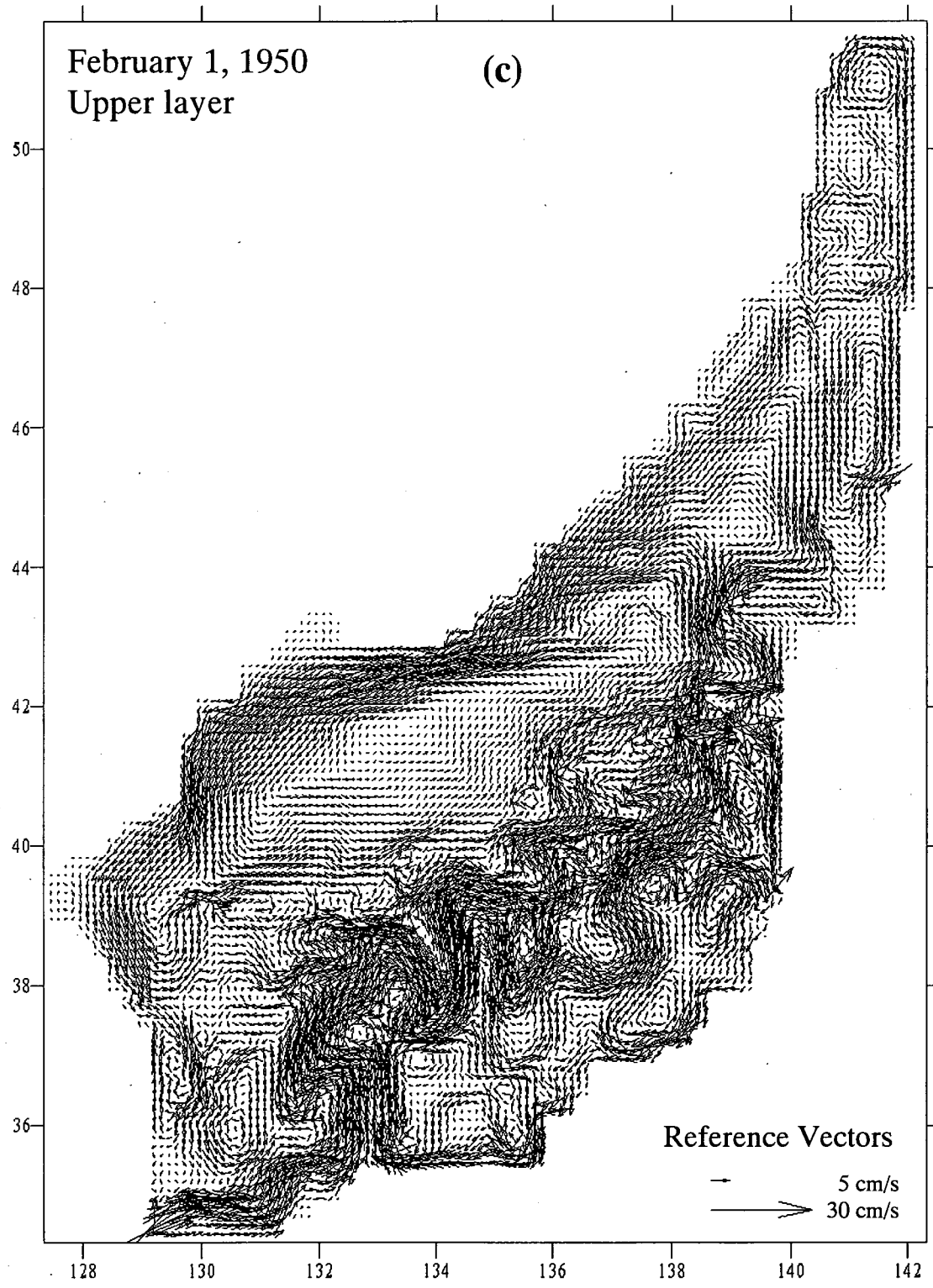

Fig.4 (continued).

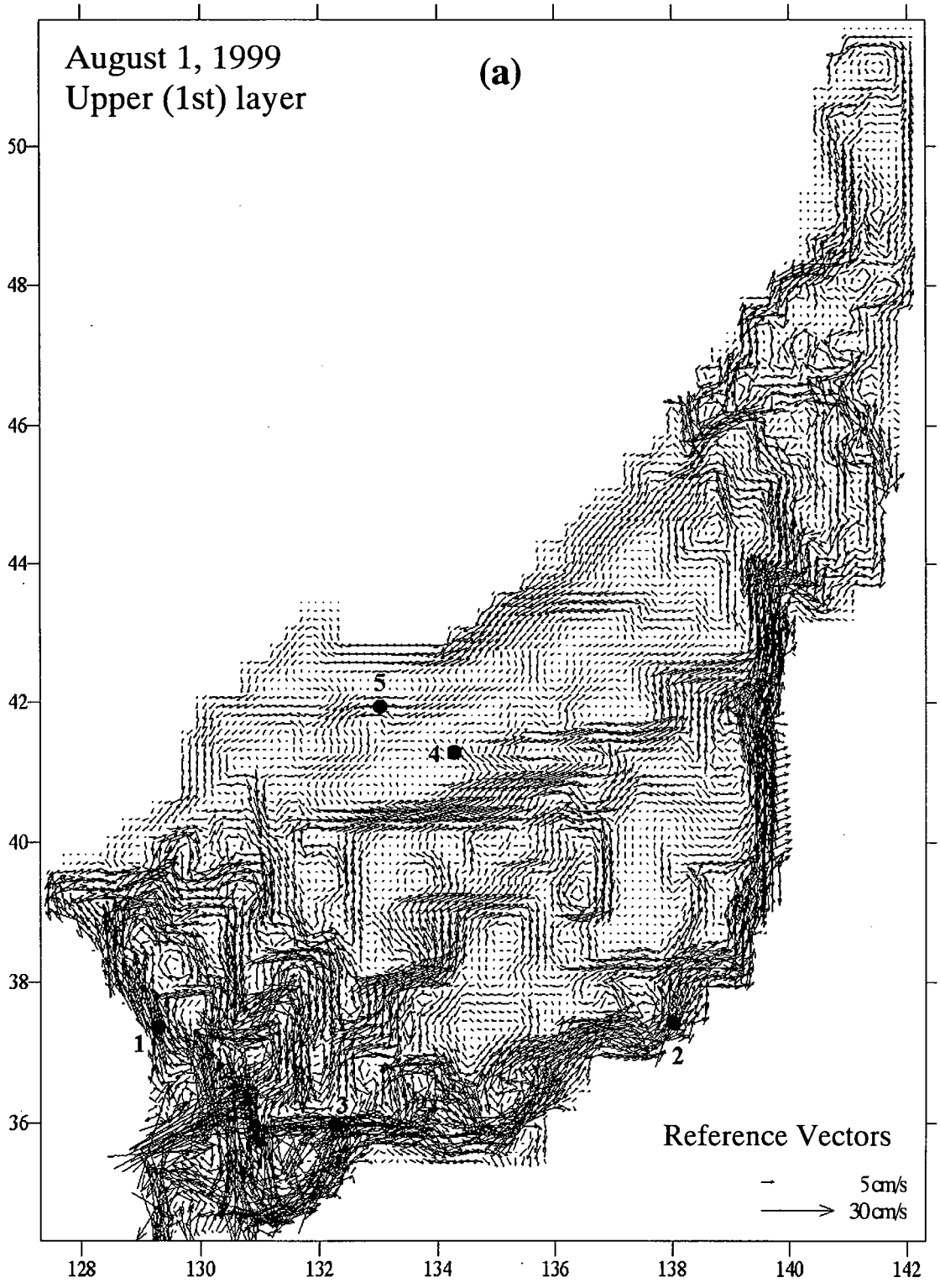

Fig. 5 The 1999 Experiment. Horizontal velocity (cm/s) for the 3rd year of integration in the upper (a) and 5th (b) layers on August 1 and in the upper layer on February 1 (c). Grid locations for vertical profiles in Fig. 8 (for 1999) are shown in (a).

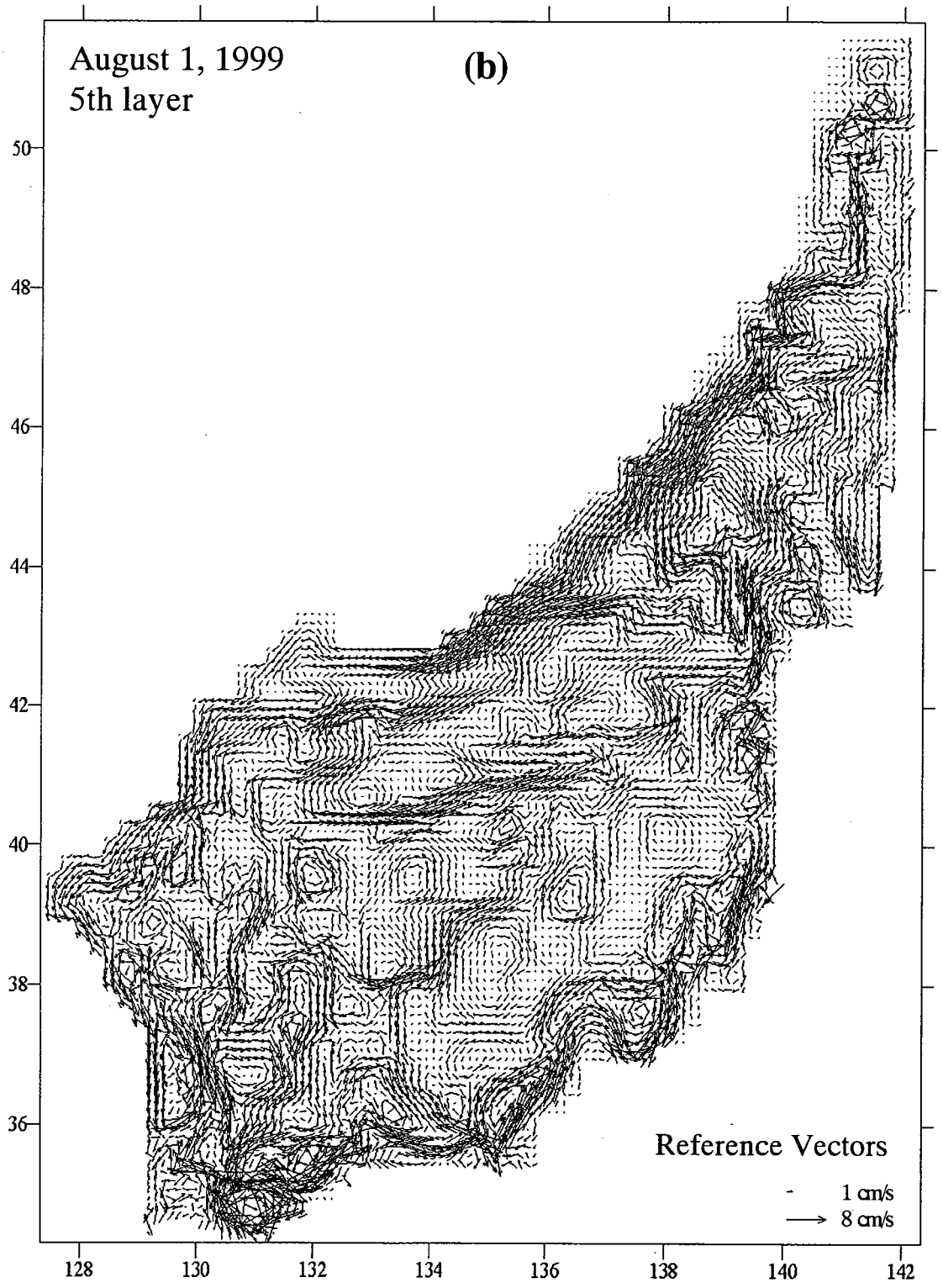

Fig.5 (continued).

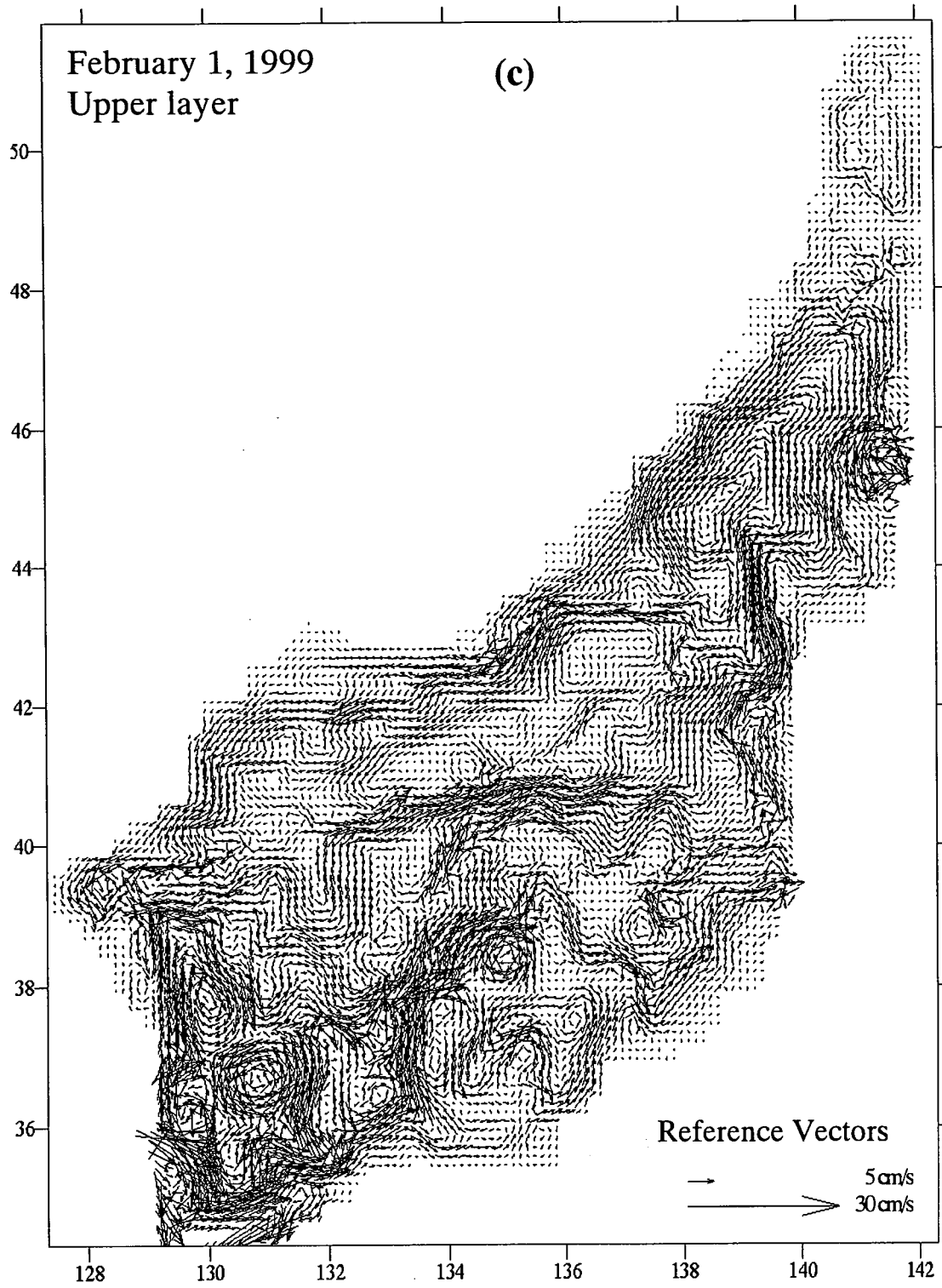

Fig.5 (continued).

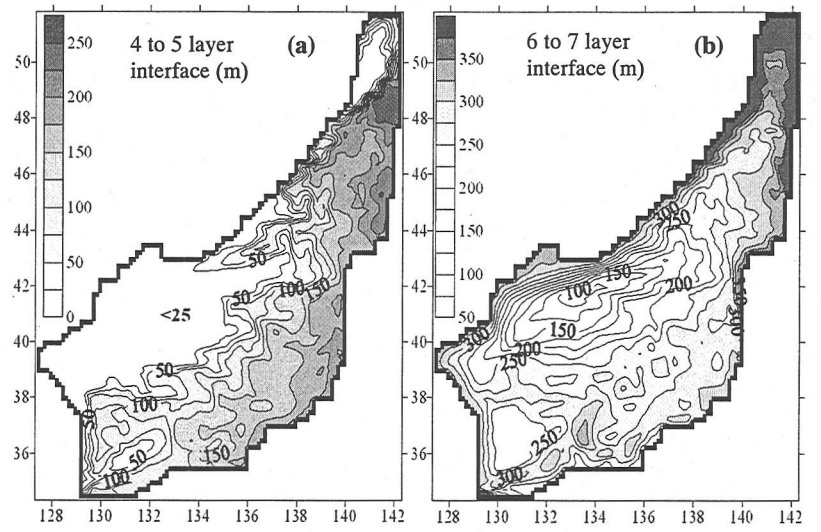

Fig. 6 The 1950 Experiment. Topography (m) of interfacial surfaces between the 4th and 5th layer that is upper portion of pycnocline (a), and between the 6th and 7th layer that is pycnocline bottom (b) in summer for the same date as in Fig.4(a),(b).

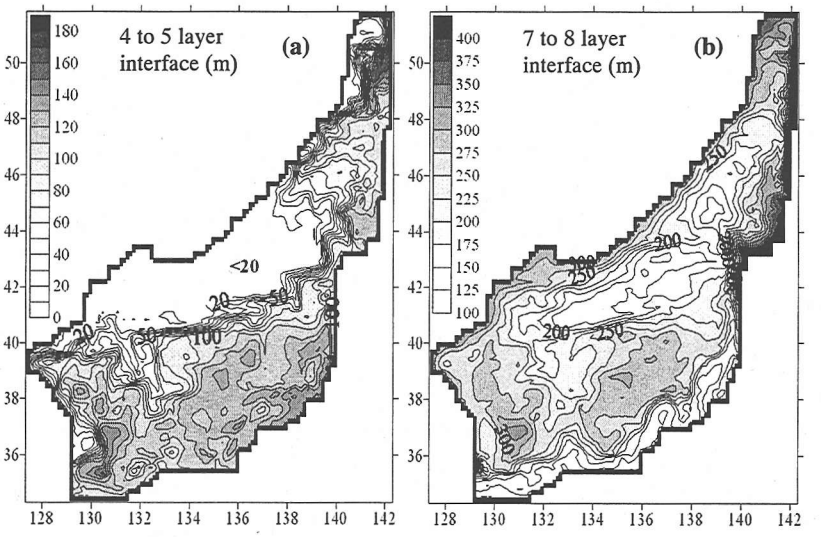

Fig. 7 The 1999 Experiment. Topography (m) of interfacial surfaces between the 4th and 5th layer that is upper portion of pycnocline (a), and between the 7th and 8th layer that is pycnocline bottom (b) in summer for the same date as in Fig. 5(a),(b).

Maximum velocity is simulated at the sea surface in the sea area adjacent to the Eastern Tsushima Channel in summer 1950. It reaches value of 61 cm/s at the location 3 from **Fig. 4a** (see the profile in **Fig. 8e**). This current is characterized by vertical shear of velocity, as seen in **Figs. 8c** and **8e** where profiles are shown at the locations 2 and 3 from **Fig. 4a**. Due to extensive transport of warm subtropical water to the southeastern Japan Sea, surface water is more buoyant there in 1950 than in 1999, as demonstrated by buoyancy profiles (**Figs. 8d** and **8f**) at the locations 2 and 3 from **Figs. 4a** and **5a**. Buoyancy reaches value of 7 cm/s^2 (**Fig. 8f**) at the location 3 in 1950. Pycnocline is sharper there in 1950 than in 1999 and vertical buoyancy gradient is very low below 60 m (in 1950; **Fig. 8f**).

In summer 1999 the simulated offshore (second) branch is formed from convergence of the inflow through the Western and Eastern Tsushima Channels and the nearshore branch develops from the inflow through the Eastern Tsushima Channel. The two branches are well separated westward of 132°E, from 133° to 136°E, and from 137° to 139°30′E but otherwise they merge (**Fig. 5a**).

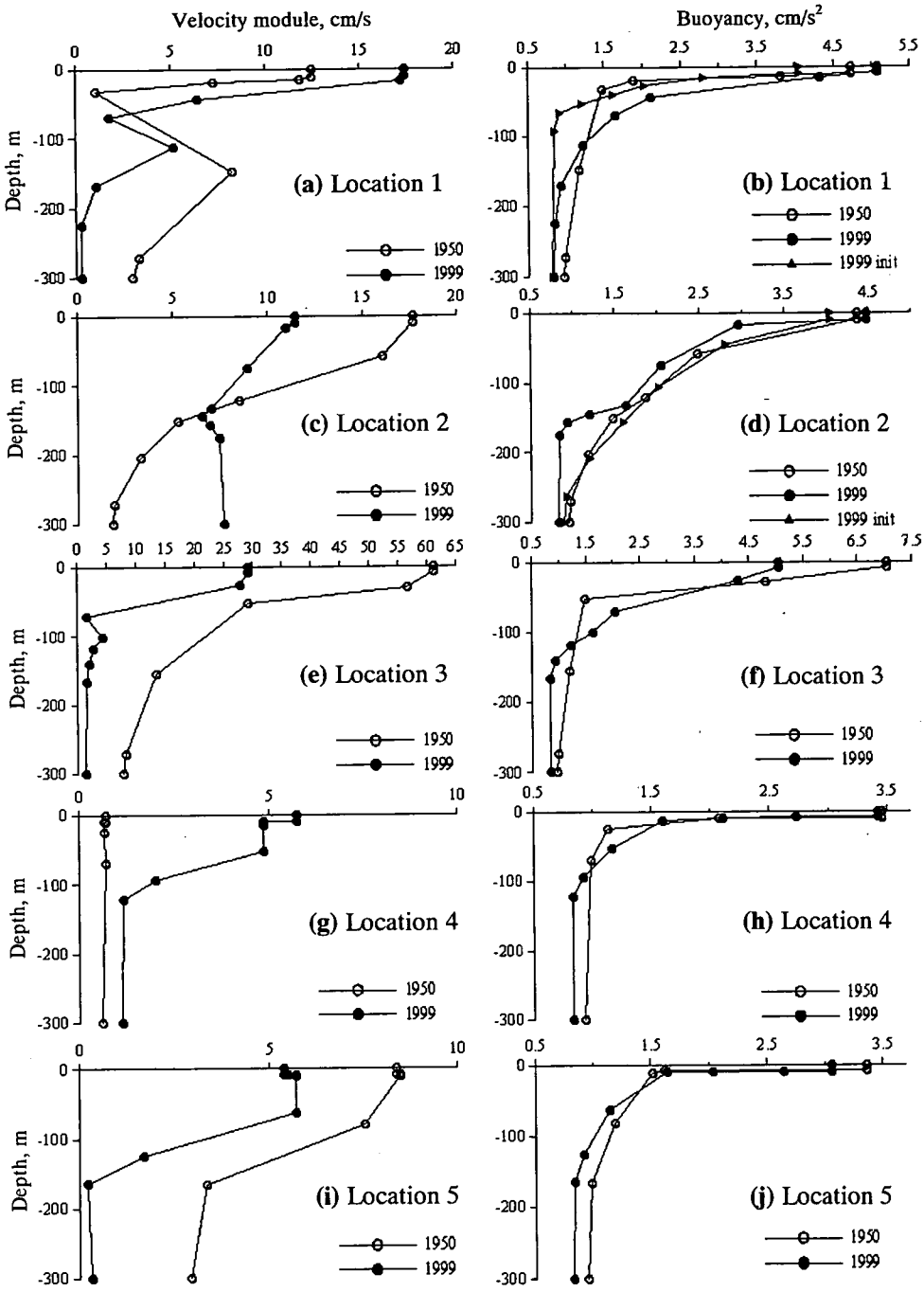

Fig. 8 Upper portion of vertical profiles (depth in m) of horizontal velocity module (cm/s) and buoyancy (cm/s^2) in grid locations within the East Korean Warm Current (a, b), nearshore (c, d) and offshore (e, f) branches of the Tsushima Current, core of the subarctic gyre (g, h), and Primorye Current (i, j) in summer 1950 and 1999 for the same dates as in Figs. 4a,b and 5a,b. Corresponding grid locations numbered from 1 through 5 are shown in Figs.4 and 5. Initial 1999 buoyancy profiles are also shown for some locations.

When separated, the nearshore branch flows close to the coast, while the offshore branch meanders, following bends of bottom topography slopes (**Figs. 1a** and **5a**). In the intermediate layer the countercurrent is simulated flowing in the southwestward direction from 40°N to the Tsushima Strait adjacent area at the western edge of the nearshore branch but below the offshore branch (**Fig. 5b**). This countercurrent is well known from observations[3].

As simulated in the 1999 experiment, the nearshore branch flows in the intermediate layer between this countercurrent and the Japanese coast (**Fig. 5b**). The highest velocity within the offshore branch simulated in the 1999 experiment is at the sea surface; it is of 30 cm/s at the location 3 from **Fig. 5a**, twice less than in 1950 (**Fig. 8e**). The offshore branch is characterized by considerable vertical shear of velocity and by secondary velocity maximum in the core of the countercurrent with value of 4.5 cm/s at 100 m depth at the profile in **Fig. 8e** for the location from **Fig. 5a**.

In contrast, vertical velocity shear is very weak within the nearshore branch, as shown at the profile for 1999 (**Fig. 8c**) at the location 2 from **Fig. 5a**. As simulated in summer 1999, sea surface height slopes up (not shown), interfaces between the upper layers, from 1st to 5th, slope down (**Fig. 7a**), and interfaces between the lower layers, from 6th and below, slope up towards the Japanese coast (**Fig. 7b**). These facts suggest that in the 1999 experiment the offshore branch is baroclinic, while nearshore branch has strong barotropic component, in agreement with observations[3]. This result is obtained despite the fact that, with the bottom topography scaling factor assumed in our experiments (see Section 2), the nearshore branch flows over deep sea with the flat bottom, while in reality it flows over the shelf, according to observations[3].

In both experiments, branches of the Tsushima Current are simulated in the central southern sea area over the Oki Bank and Yamato Rise. In 1950 the simulated Tsushima Current forms an anticyclonic meander and eddy (with horizontal dimensions of 40×80 km) over the Oki Bank and splits, with portion of the flow turning southeastward and merging with the nearshore branch (**Fig. 4a**). The other portion flows northeastward, with jets of the EKWC Extension joining it, and meanders over the Yamato Rise. Both cyclonic and anticyclonic eddies (with horizontal dimensions of 40–100 km) develop over the Tsushima Basin in the upper layer and pycnocline (**Figs. 4a** and **4b**). Their signature is seen in topography of the interface between the 6th and 7th layers (**Fig. 6b**). Cyclonic and anticyclonic eddies are documented in the southeastern Japan Sea from remotely sensed sea surface temperature[11].

In winter 1950 the simulated Tsushima Current meanders over the Yamato Rise and Yamato Basin (**Fig. 4c**), consistent with a "single-meander-path" pattern[6]. In summer 1999 the northward central branch is simulated over the Oki Bank and Yamato Rise. A portion of it turns clockwise to the southeast and merges with the first and second branches, with anticyclonic mesoscale eddies developing at the right-hand side of the flow (**Fig. 5a**). This pattern is consistent with the Loop Path reported from analysis of infrared imagery[18].

(2) Circulation change in the northwestern Japan Sea

In both 1950 and 1999 experiments, the cyclonic gyre is simulated in the northern Japan Sea and Tatarsky Strait, with cold currents flowing south- and southwestward along the western sea boundary. They are the North Korea Cold Current (NKCC) along the North Korea coast and Primorye (Liman) Current along the Primorye (Siberian) coast (**Figs. 4** and **5**). The subarctic gyre is clearly seen in topography of interfacial surfaces as an elevation in the northern and northwestern Japan Sea extending to the Tatarsky Strait (**Figs. 6** and **7**). The cyclonic gyre expands southward by 1°-2° in winter, compared to summer (compare **Fig. 4a** with **Fig. 4c** and **Fig. 5a** with **Fig. 5c**). In pycnocline the NKCC follows further south along the coast as a countercurrent underneath the EKWC, as was discussed above.

In the upper layer the simulated NKCC turns eastward at 38°N in 1950 (**Fig. 4a**) and at 41°N in 1999 (**Fig. 5a**) and separates off the coast, forming the northern subarctic front, in agreement with observations[7]. In the 1999 experiment, anticyclonic circulation associated with the EKWC develops in the northwestern Japan Sea, while the cyclonic gyre is shifted northeastward and countercurrent in the intermediate layer is weak (**Fig. 5**). Development of anticyclonic eddies both in the upper layer and pycnocline have been reported in many studies, based on satellite imagery and ship measurements in the northwestern Japan Sea[13),14),15),17),31].

In the subarctic area, simulated pycnocline is much thinner than in the subtropical area. Inside the subarctic gyre depth of pycnocline bottom can be estimated as 60–70 m for the 1950 experiment and 100–120 m for the 1999 experiment, as shown in vertical buoyancy profiles (**Fig. 8h**). Within the Primorye (Liman) Current there is no noticeable difference in vertical stratification between the 1950 and 1999 experiments: thermocline bottom lies at about 160 m in both cases (**Fig. 8j**). Accordingly, in the subarctic area simulated velocity sharply drops from the sea surface down to 100–120 m, while there is almost no vertical velocity shear below

(**Figs. 8g** and **8i**). In contrast, in the subtropical area considerable velocity shear is simulated from the surface down to 200–250 m depth due to deeper pycnocline (**Figs. 8a**, **8c**, and **8e**).

In 1950 the simulated subarctic gyre is intensified and velocity of the cold currents at its western edge is higher, compared to 1999. This is clearly seen from the comparison of velocity fields (**Figs. 4** and **5**) and also from the vertical velocity profiles at the location 5 (**Fig. 8i**) within the Primorye Current: in summer velocity in the upper 10 m layer is 8.5 cm/s for the 1950 Experiment, while it is 5.4–5.8 cm/s for the 1999 Experiment (**Fig. 8i**). In the lower layer simulated velocity is of 0.5–1 cm/s. This is in line with observational evidence: velocity of 1–10 cm/s at depths of 1000–3000 m is reported for deep currents based on mooring data[16].

The subarctic frontal zone separating the southern (subtropical) and northern (subarctic) sea areas is simulated in both experiments (**Figs. 4** and **5**). The southern (northern) front manifests itself by sharp gradients in topography of interfacial surfaces between the 4th and 5th (6th and 7th for 1950 or 7th and 8th for 1999) layers, respectively (**Figs. 6** and **7**). The northern subarctic front extends to the northern sea area and Tatarsky Strait in both experiments, in agreement with observational evidence[7]. Branches of the EKWC Extension turn westward between 43°–36°N, as simulated in both experiments (**Figs. 4** and **5**).

In 1950 the simulated subarctic frontal zone is stretched out along 38°–39°N in the western Japan Sea (westward 133°E) and in direction from southwest to northeast in the eastern area, as seen in velocity (**Fig. 4**) and interface topography (**Fig. 6**). The cyclonic circulation prevails in the northwestern sea area. In 1999 the simulated EKWC is intensified and propagates farther north, as was discussed above. Respectively, the subarctic frontal zone is oriented in the direction from northwest to southeast in the northwestern Japan Sea, as seen in velocity field (**Fig. 5**) and interface topography (**Fig. 7**). This is in line with thermal surface fronts reported from ship measurements and multiple infrared satellite images of this area in late 1990s[8),17),31)]. As a result of the intensified EKWC, the anticyclonic circulation prevails in the northwestern Japan Sea, where anticyclonic meanders, filaments, and rings of the EKWC develop throughout the year, with seasonal southward shift in winter (**Fig. 5**).

Dimensions of simulated EKWC rings are of about 60–80 km, in the upper layer and pycnocline, in agreement with observations[10),12),13),17)]. Their signature is present in topography of interfacial surfaces between intermediate layers (**Fig. 7a**). Warm eddies are considered as an important source of northward heat transport through the eddy streets device. For the northwestern Japan Sea it was suggested by Danchenkov et al.[15].

In summer 1999 simulated eddy streets are clearly seen as tongues of anticyclonic (negative) relative vorticity in the upper layer (**Fig. 9a**). At least three eddy streets are stretched out in northeastward direction in the western sea area (westward 133°E) and reach as far north as 41°N. One more eddy street is simulated in the central sea over the Oki Bank and Yamato Rise (along 133°–134°E; **Fig. 9a**). It is located within the central branch of the Tsushima Current or Loop Path[18]. The eddy streets in the western and central sea can be also seen in the relative vorticity distribution in winter 1999 (not shown). In contrast, cyclonic (positive) vorticity prevails in this area in 1950 (**Fig. 9b**).

A specific feature of the simulated cyclonic gyre is its multi-core structure, as seen in the velocity field both in the 1950 and 1999 experiments (**Figs. 4** and **5**). The cyclonic sub-gyres and mesoscale cores manifest themselves as elevations in topography of interfaces between the intermediate layers (**Figs. 6** and **7**). Observational evidence on system of cyclonic gyres in the northern Japan Sea is presented by Yurasov and Yarichin[2]. Splitting of the cyclonic gyre can be associated with irregularity in shape and depth of the Japan Basin. The largest sub-gyre is located between 41°N and 43°N off the Russian coast (**Figs. 4**, **5**, and **10**). Its northeastern edge is formed by the westward branch of the EKWC Extension. It is simulated in both numerical experiments, in the upper layer and pycnocline, in summer and in winter (**Figs. 4**, **5**, and **10**).

The cyclonic gyre at 41°– 43°N and westward currents off the Tsugaru Strait were reported, based on PALACE floats drift, both in upper and deep layers[9]. The multi-core structure of the subarctic gyre and westward jet currents have already been simulated by the MHI model in the low resolution 1999 Experiment and in the long-term run from flat interfaces[32].

Mesoscale cyclonic cores develop inside the gyre at 41°– 43°N, associated with depressions in the Japan Basin bottom topography (**Fig. 10**). Their dimensions are of 50–80 km (4–8 times more than grid size); in summer 1999 they are centered at (131°30′E, 41°30′N), (132°45′E, 40°45′N), (134°20′E, 41°N), (134°50′E, 41°50′N), (136°E, 42°30′N), (136°45′E, 43°N), and (138°40′E, 44°30′N), as seen in **Fig. 10**.

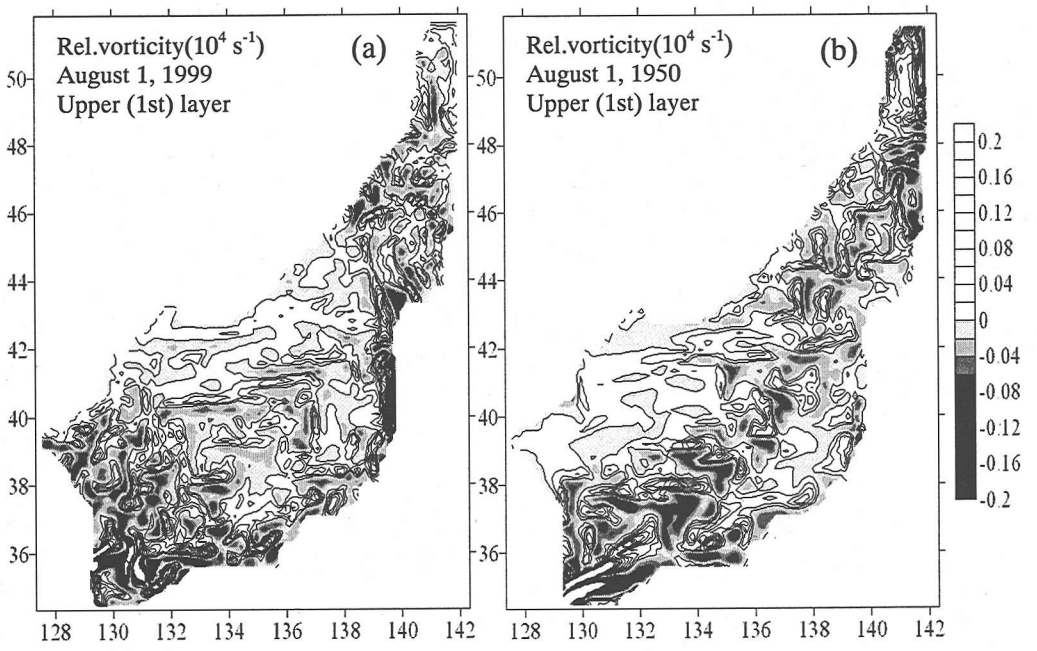

Fig. 9 Relative vorticity (multiplied by $10^4 \times s^{-1}$) in the 1st (upper) layer for the 1999 (a) and 1950 (b) Experiments in summer for the same dates as in Figs. 5(a) and 4(a), respectively. Anticyclonic vorticity is negative (shaded) and cyclonic vorticity is positive (in white).

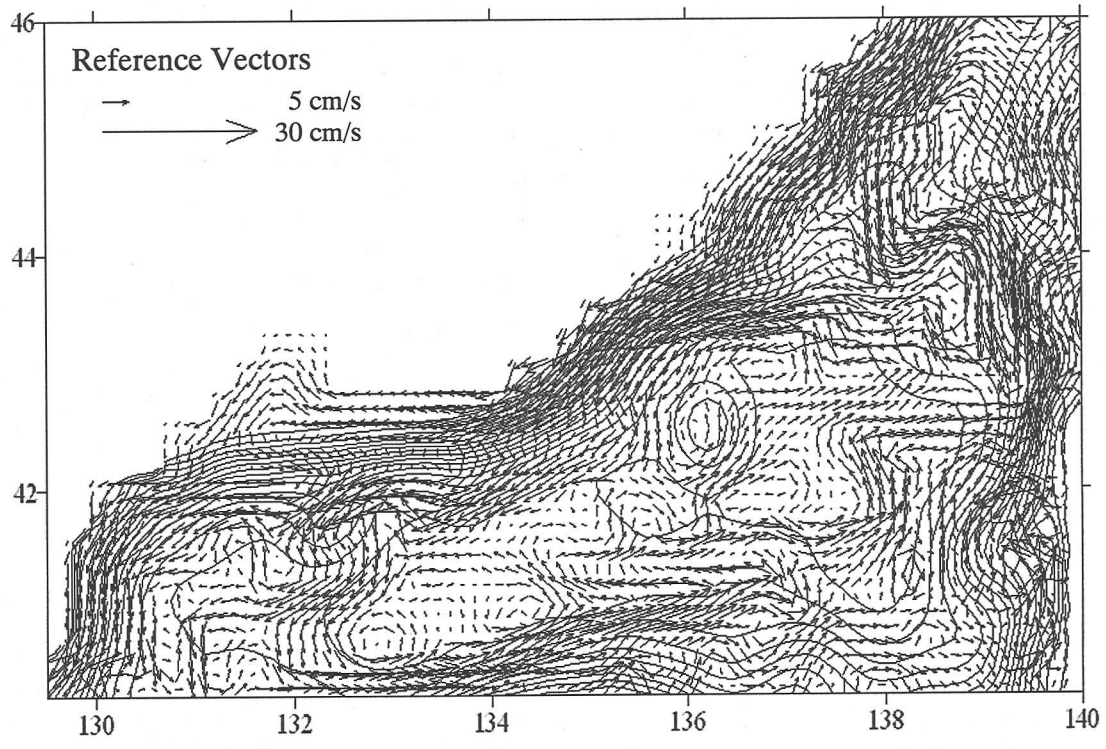

Fig. 10 The 1999 Experiment. Zoomed view of the area off Vladivostok: horizontal velocity (cm/s; arrows) in the 5th layer in sum mer, for the same date as in Fig. 5(a), and model bottom topography (m; contours every 100 m).

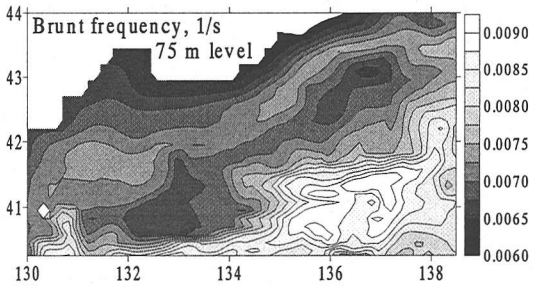

Fig. 11 The 1999 Experiment. Brunt frequency (s^{-1}) interpolated on the 75 m level in summer for the same date as in Fig. 3(a),(b) and for the same area as in Fig. 10.

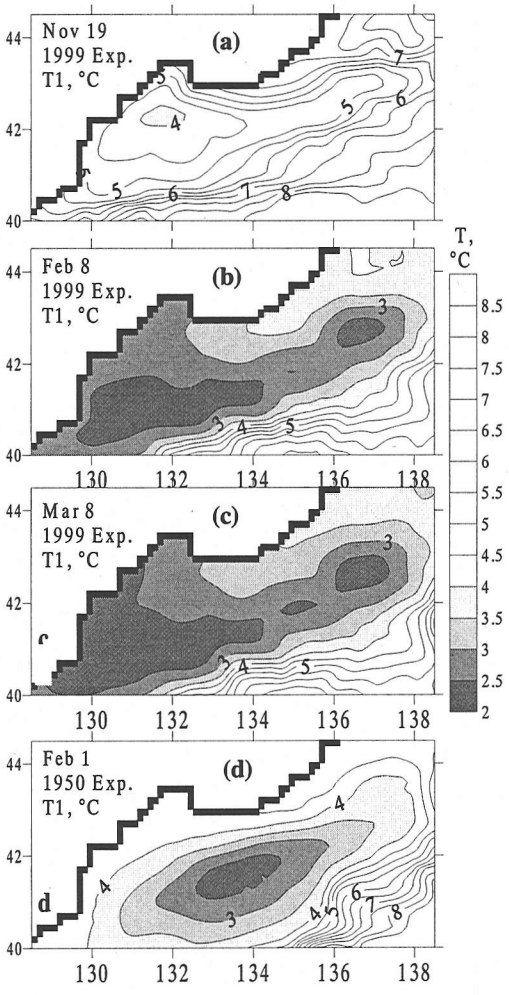

Fig. 12 Wintertime temperature (°C) in the upper layer on the 3rd year of integration for the same area as in Fig. 10 for 1999(a), (b), (c) and 1950 (d). Contours are shown every 0.5°C.

A similar chain of low temperature cores can be seen between 41°N and 42°N (westward 135°E) at the infrared NOAA AVHRR image on October 3, 1999 (Personal communication from Dr. Lobanov). In the 1999 Experiment, the simulated Primorye Current at the northwestern edge of the 42°– 43°N cyclonic gyre splits over the continental slope, developing an anticyclonic meander and southward jet over the Siberia Seamount off Vladivostok (**Fig. 10**).

The westward branch of the EKWC Extension brings warm subtropical water to Peter the Great adjacent area from the east. This is especially evident in the 1999 Experiment. To demonstrate this Brunt frequency is calculated from vertical buoyancy profiles and interpolated to the flat level of 75 m in depth. Brunt frequency is increased in pycnocline where vertical density gradient is high and decreased above and below it. In the area shown in **Fig. 11**, Brunt frequency is highest at its southeastern corner where the warm EKWC Extension flows, characterized by deeper pycnocline. Inside the cold cyclonic gyre of the northwestern Japan Sea, Brunt frequency is decreased, as the sharpest vertical density gradient lies on the 75 m level (**Fig. 11**). Minimum values are located in the cores of the subarctic gyre at (132°45′E, 40°45′N), (136°E, 42°30′N), and (136°45′E, 43°N). Brunt frequency is also decreased in the coastal area where the cold Primorye (Liman) Current flows (**Fig. 11**). A tongue of increased Brunt frequency is stretched out between the cyclonic gyre interior and the Primorye Current water. It can be associated with the westward branch of the EKWC Extension with deeper pycnocline.

During the cold period of a year simulated temperature in the upper layer reaches its lowest values in the cores of the cyclonic gyre (**Fig. 12**). Temperature is higher at the periphery of the gyre, including its northwestern margin adjacent to the Russian coast. In the 1999 Experiment, a tongue of warmer water spreads as far west as Peter the Great Bay area (132°E; **Figs. 12b** and **12c**). In 1950 warmer water spreads no farther west than 134°E (**Fig. 12d**).

4. CONCLUSIONS

Substantial difference of the Japan Sea circulation is revealed in conditions of decreased or increased baroclinicity, associated with both seasonal variations and climatic regime change. The MHI model was integrated up to 3 years, so the circulation is, to some extent, still associated with initial condition of integration but not entirely determined by it, as density field is modified by buoyancy forcing and dynamic factor. As inflow at the Tsushima Strait is

intentionally taken the same in both cases, the only external factor which conditions the circulation change is difference in heat exchange through the sea surface. This effect is especially important in the northwestern Japan Sea where climate change is most pronounced and pycnocline is very thin. The principal conclusions are as follows.

(1) The inflow transport at the Tsushima Strait is redistributed between the western and eastern branches of the Tsushima Current in such a way that the EKWC (western branch) is intensified in conditions of increased baroclinicity (in summer and/or in late 20th century) and the eastern branches are intensified in conditions of decreased baroclinicity (in winter and/or in the mid 20th century). Seasonal variation is supported by observational evidence[4] and is consistent with simulation of currents in the Tsushima Strait using hydraulic model[5].

(2) The intensification of the EKWC is accompanied by deepening of pycnocline in the adjacent area. The increased barotropy of the first (nearshore) branch of the eastern Tsushima Current in 1999 may be associated with redistribution of mass flux and kinetic energy in favor of the western branch (EKWC).

(3) The central branch of the Tsushima Current is simulated in the southern Japan Sea over the Yamato Rise, regardless of initial condition. It corresponds to the Loop Path of the Tsushima Current in the central sea area[18] and eddy street along 134°N observed at satellite images[15].

(4) In the subarctic area of thin pycnocline large-, mid-, and mesoscale circulation patterns over irregular bottom topography are obtained in both simulations. The simulated cyclonic gyre and cold currents at its northwestern edge are intensified in 1950. In contrast, in the climatic regime of late 20th century, anticyclonic meanders and rings of the EKWC are simulated in the northwestern Japan Sea.

(5) As simulated for climatic conditions of the mid 20th century, the subarctic front in the northwestern Japan Sea is stretched out along 39°N in zonal direction, as in most simulation results[22),23),26)] and in traditional circulation schemes[2]. In the mid 20th century the northwestern branch of the subarctic front is stretched out from the North Korea – Russian coast in the southeastward direction in agreement with observational evidence based on satellite images and ship measurements[8),13),14),15)].

(6) As simulated by the MHI model for two climatic regimes, the northwestern Japan Sea is substantially warmer in 1999, compared to 1950. Warm water is transported to this area from the southwestern and central Japan Sea by mesoscale jets associated with warm currents in the subtropical area. This is consistent with the eddy street device of heat transport in the Japan Sea[15]. Subtropical water is also transported to the northwestern Japan Sea from the east with the westward branch of the EKWC Extension.

REFERENCES

1) Leonov, A.K.: *Regional Oceanography, Part I*, Gidrometeoizdat, Moscow, Russia, 1960 (in Russian).
2) Yurasov, G.I., and Yarichin, V.G.: *Currents of the Japan Sea*, Dalnauka Publishing House, Vladivostok, Russia, 1991 (in Russian).
3) Hase, H., Yoon J.H., and Koterayama, W.: The current structure of the Tsushima Warm Current along the Japanese coast, *J. Oceanogr.*, Vol. 55, No.2, pp. 217-235, 1999.
4) Kim, K., and Legeckis, R.: Branching of the Tsushima Current in 1981 – 1983, *Progress of Oceanography*, Vol. 17, pp. 265-276, 1986.
5) Cho, Y.K., and Kim, K.: Branching Mechanism of the Tsushima Current in the Korea Strait, *J. Phys. Oceanogr.*, Vol. 30, pp. 2788-2797, 2000.
6) Katoh, O.: Structure of the Tsushima Current in the southwestern Japan Sea, *J. Oceanogr.*, Vol. 50, pp. 317-338, 1994.
7) Zuenko, Yu.I.: Two decades of Polar Front large-scale meandering in the North-western Japan Sea, *Proc. of the CREAMS'99 Int. Symp., Fukuoka, Japan*, pp. 68-71, 1999.
8) Danchenkov, M.A., Nikitin, A.A., Volkov, Yu. N. and Goncharenko, A.A.: Surface thermal fronts of the Japan Sea, *Proc. CREAMS'97 Int. Symp., January 26-31, 1997, Fukuoka, Japan*, pp. 75-80, 1997a.
9) Danchenkov, M.A., and Riser, S.C.: Observation of currents, temperature and salinity in the Japan Sea in 1999-2000 by PALACE floats, *Oceanography of the Japan Sea, Proc. of CREAMS'2000 International Symposium*, Danchenkov, M.A., ed, Dalnauka Publishing House, Vladivostok, Russia, pp. 33-40, 2001.
10) Ichiye, T., and Takano, K.: Physical structure of eddies in the Southwestern East Sea, *La Mer*, Vol. 26, pp. 69-75, 1988.
11) Isoda, Y.: Warm eddy movements in the Eastern Japan Sea, *J. Oceanogr.*, Vol. 50, pp. 1-16, 1994.
12) Isoda, Y., and Saitoh, S.: The northward intruding eddy along the East coast of Korea, *J. Oceanogr.*, Vol. 49, pp. 443-458, 1993.
13) Ginzburg, A.I., Kostianoy, A.G., and Ostrovskii, A.G.: Surface circulation of the Japan Sea (satellite information and drifters data), *Earth Research from Space* (Issledovanie Zemli iz Kosmosa), Vol. 1, pp. 66-83, 1998 (in Russian).
14) Shin, C.-W., Byun, S.-K., Kim, C., and Seung, Y.H.: Warm core in the East Korean Bay in winter, *Oceanography of the Japan Sea, Proc. of CREAMS'2000 International Symposium*, Danchenkov, M.A., ed, Dalnauka Publishing House, Vladivostok, Russia, pp. 104-111, 2001.
15) Danchenkov, M.A., Lobanov, V.B., and Nikitin, A.A.: Mesoscale eddies in the Japan Sea, their role in circulation and heat transport, *Proc. CREAMS'97 Int. Symp., January 26-31, 1997, Fukuoka, Japan*, pp. 81-84, 1997.
16) Takematsu, M., Ostrovskii, A.G., and Nagano, Z.: Observations of eddies in the Japan Basin interior, *J. Oceanography*, Vol. 55, No.2, pp. 237-246, 1999.
17) Lobanov, V.B., Ponomarev, V.I., Tishchenko, P.Y., Talley, L.D., Mosyagina, S.Y., Sagalaev, S.G., Salyuk, A.N., and Sosnin, V.A.: Evolution of anticyclonic eddies in the northwestern Japan/East Sea, *Extended abstracts of 11th PAMS/JECSS Workshop, Cheju, Korea, April 11-13, 2001*, pp. 37-40, 2001.

18) Ostrovskii, A., and Hiroe, Y.: The Japan Sea circulation as seen in satellite infrared imagery in autumn 1993, *Proc. CREAMS'94, 24-26 Jan. 1994, Fukuoka, Japan*, pp. 129-133, 1994.
19) Ponomarev, V.I., Kaplunenko D.D., and Ishida, H.: The 20th century climate change in the Asian-Pacific Region, *Oceanography of the Japan Sea, Proc. of CREAMS'2000 International Symposium*, Danchenkov, M.A., ed, Dalnauka Publishing House, Vladivostok, Russia, pp. 129-136, 2001.
20) Ponomarev, V.I., and Salyuk A.N.: The climate regime shifts and heat accumulation in the Sea of Japan, *Proc. CREAMS'97 Int. Symp., January 26-31, 1997, Fukuoka, Japan*, pp. 75-80, 1997.
21) Yoon, J.-H.: The branching of the Tsushima Current, *Rep. Res. Inst. Appl. Mech. Kyushyu Univ.*, Vol. 38, pp. 1-21, 1991.
22) Kim, C.-H., and Yoon, J.H.: A numerical modeling of the upper and the intermediate layer circulation in the East Sea, *J. Oceanogr.*, Vol. 55, No.2, pp. 327-345, 1999.
23) Hogan, P.J., and Hurlburt, H.E.: Impact of upper ocean-topographic coupling and isopycnal outcropping in Japan/East Sea models with 1/8° to 1/64° resolution, *J. Phys. Oceanogr.*, Vol. 30, pp. 2535-2561, 2000.
24) Seung, Y.H., and Kim, K.: On the possible role of local thermal forcing on the Japan Sea circulation, *J. Oceanological Society Korea*, Vol. 24, No.1, pp. 29-38, 1989.
25) Seung, Y.H.: A simple model for separation of East Korean Warm Current and formation of North Korean Cold Current, *J. Oceanological Society Korea*, Vol. 27(3), pp. 189-196, 1992.
26) Kim, K.-J., and Seung, Y.H.: Formation and movement of the ESIW as modeled by MICOM, *J. Oceanogr.*, Vol. 55, No.2, pp. 369-382, 1999.
27) Shapiro, N.B.: Formation of the Black Sea general circulation considering stochastic wind stress, *Marine Hydrophysical Journal (Morskoy Gidrofisicheskii Journal)*, Sebastopol, Ukraine, Vol. 6, pp. 26-40, 1998 (In Russian).
28) Bleck, R., Hanson, H.P., Hu, D. and Kraus, E.B.: Mixed layer-thermocline interaction in a three-dimensional isopicnic coordinate model, *J. Phys. Oceanogr.*, Vol. 19, No.10, pp. 1417-1439, 1989.
29) Semtner, A.J., and Mintz, Y.: Numerical simulations of the Gulf Stream and mid-ocean eddies, *J. Phys. Oceanogr.*, Vol. 7, pp. 208-230, 1977.
30) Lie, H.-J., and Cho, C.-H.: On the origin of the Tsushima Warm Current, *J. Geophys. Res.*, Vol. 99, No.C12, pp. 25081-25091, 1994.
31) Trusenkova, O.O., Ponomarev, V.I., and Lobanov, V.B.: The Japan/East Sea circulation features associated with the climatic regimes of 1950s and 1990s, *Extended abstracts of 11th PAMS/JECSS Workshop, Cheju, Korea, April 11-13, 2001*, pp. 301-304, 2001.
32) Ponomarev, V.I., Trusenkova, O.O., and Talley, L.D.: Simulation of the Japan Sea circulation in summer 1999 using the MHI layered model, *Oceanography of the Japan Sea, Proc. of CREAMS'2000 International Symposium*, Danchenkov, M.A., ed, Dalnauka Publishing House, Vladivostok, Russia, pp. 104-111, 2001.

(Received April 9, 2002)